AD-A087 449 CORNELL UNIV ITHACA NY SCHOOL OF APPLIED AND ENGINEE--ETC F/6 20/10
HIGH QUALITY SUBMICRON NIOBIUM TUNNEL JUNCTIONS WITH REACTIVE I--ETC(U)
JUL 80 A W KLEINSASSER, R A BUHRMAN N00014-76-C-0526

UNCLASSIFIED 80-4 NL

1 of 1

END
DATE
FILMED
9-80
DTIC

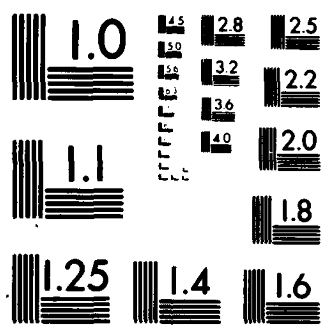

MICROCOPY RESOLUTION TEST CHART

UNCLASSIFIED

SECURITY CLASSIFICATION OF THIS PAGE (When Data Entered)

LEVEL II

ADA087449

REPORT DOCUMENTATION PAGE		READ INSTRUCTIONS BEFORE COMPLETING FORM
1. REPORT NUMBER (14) 80-4	2. GOVT ACCESSION NO. AD-A087449	3. RECIPIENT'S CATALOG NUMBER
4. TITLE (and Subtitle) (6) High Quality Submicron Niobium Tunnel Junctions with Reactive Ion Beam Oxidation.		5. TYPE OF REPORT & PERIOD COVERED (9) Technical Report.
		6. PERFORMING ORG. REPORT NUMBER 80-4
7. AUTHOR(s) (10) Alan W. Kleinsasser & Robert A. Buhrman		8. CONTRACT OR GRANT NUMBER(s) NR 319-096
9. PERFORMING ORGANIZATION NAME AND ADDRESS R. A. Buhrman, Appl. & Engineering Physics Cornell University Ithaca, New York 14853	(15)	10. PROGRAM ELEMENT, PROJECT, TASK AREA & WORK UNIT NUMBERS N00014-76-C-0526
11. CONTROLLING OFFICE NAME AND ADDRESS Electronic & Solid State Sciences Program Code 427 - Office of Naval Research 800 N. Quincy, Arlington, VA 22217	(11) 22	12. REPORT DATE July 1980
		13. NUMBER OF PAGES 14
14. MONITORING AGENCY NAME & ADDRESS(if different from Controlling Office) (12) 15		15. SECURITY CLASS. (of this report) Unclassified
		15a. DECLASSIFICATION/DOWNGRADING SCHEDULE

16. DISTRIBUTION STATEMENT (of this Report)

Approved for public release, distribution unlimited.

DTIC ELECTE AUG 5 1980 S D

17. DISTRIBUTION STATEMENT (of the abstract entered in Block 20, if different from Report)

D

18. SUPPLEMENTARY NOTES

19. KEY WORDS (Continue on reverse side if necessary and identify by block number)

Superconducting Magnetometers, rf SQUIDs, SQUID noise

20. ABSTRACT (Continue on reverse side if necessary and identify by block number)

A new reactive ion beam oxidation tehcnique has been applied to the fabrication of rugged, high quqlity niobium-lead alloy Josephson tunnel junctions. Control of critical current density over a wide range is possible, and critical current densities exceeding 10^{6} amp/cm^{2} have been obtained. In addiiton, a process-compatible edge geometry has been developed which allows a junction to be formed on the faceted edge of a niobium base electrode, yielding devices with areas of 10^{-9} cm^{2} using 1 μm photolithography.

DD FORM 1 JAN 73 1473 EDITION OF 1 NOV 65 IS OBSOLETE S/N 0102-LF-014-6601

UNCLASSIFIED

SECURITY CLASSIFICATION OF THIS PAGE (When Data Entered)

407244

80 8 1 025

DDC FILE COPY

80-1

HIGH QUALITY SUBMICRON NIOBIUM TUNNEL JUNCTIONS WITH REACTIVE ION BEAM OXIDATION*

A. W. Kleinsasser and R. A. Buhrman
School of Applied and Engineering Physics
and
Materials Science Center
and
National Research and Resource Facility for Submicron Structures
Cornell University
Ithaca, New York 14853

ABSTRACT

A new reactive ion beam oxidation technique has been applied to the fabrication of rugged, high quality niobium-lead alloy Josephson tunnel junctions. Control of critical current density over a wide range is possible, and critical current densities exceeding 10^6 amp/cm^2 (1 million ... sq cm) have been obtained. In addition, a process-compatible edge geometry has been developed which allows a junction to be formed on the faceted edge of a niobium base electrode, yielding devices with areas of 10^{-9} cm^2 using 1 μm photolithography.

micrometer

10 to the minus 9th power sq cm

A

The attainment of high critical current densities (J_c) in Josephson tunnel junctions allows reduction of R_C time constants and hysteresis in the IV characteristics, important considerations for many potential applications. Progress in the fabrication of such devices has recently been reported[1]. Another important consideration for device applications is durability. In this respect, Nb is the best currently available material for tunnel junction devices[2]. Junctions with Nb base electrodes and Pb alloy counterelectrodes have proven to be significantly more durable than all Pb alloy junctions, and such junctions currently exhibit better device characteristics than do all Nb junctions[3,4].

The quality of a Josephson tunneling device depends critically upon the oxide barrier and its interfaces with the superconducting films. In the case of Nb-Pb alloy devices, the interface between the Nb base electrode and the Nb_2O_5 barrier oxide, including any lower oxides which may be present, tends to limit device performance. Of the available techniques, the rf plasma oxidation method[5] has been shown, under proper conditions, to yield the most controllable high quality devices[6,7]. The limitation of this technique is scattering, in the glow discharge, of cathode material and impurities which greatly affect junction properties. We have introduced a method which uses a low pressure reactive ion beam to grow the oxide barrier[8]. This technique allows control of critical current density J_c over a wide range (<1 to > 10^6 amp/cm^2)

and yields junctions with excellent single-particle tunneling characteristics.

Junctions are fabricated on rf sputtered Nb films having resistance ratios (R_{300K}/R_{10K}) of about 3 and transition temperatures of 9.2K. Base electrode patterning is done by chemical etching and ion milling. Counterelectrodes are defined using photolithography with AZ 1350J resist and are patterned by lift-off. Typical junction areas are $2 \times 10^{-8} cm^2$. Oxidation and counterelectrode deposition are carried out with the substrate held at 77K. The base electrode is first cleaned with an argon beam (600 eV, 150 $\mu A/cm^2$) and then the oxide layer is grown in an argon-oxygen beam (10-35% O_2, 2-150 $\mu A/cm^2$). The counter-electrode (ε - PbBi[9]) is evaporated immediately following oxidation.

Junction areas can easily be reduced by a factor of 10 or more if a junction can be formed on the edge of the base electrode film[1,10]. We have developed a durable edge geometry which is compatible with our fabrication process. The edge junction process is illustrated in figure 1. Except for the step of forming the tapered edge, edge junctions are fabricated by the same method as ordinary junctions. In particular, the process is compatible with lithographic and etching procedures and with film storage between steps.

Junctions with small current densities ($J_c \leq 10^4$ amp/cm^2) exhibit the familiar hysteretic IV behavior usually associated with oxide barrier tunnel devices (Figure 2). I_cR_N (R_N is the resistance of voltages well above the gap) products of 1.8 mV were obtained. This is somewhat below the theoretical prediction of 2.5 mV[11] (obtained from the measured energy gaps of 3.0 and 3.4 meV of the Nb and PbBi films). This reduction is familiar in Nb-Pb alloy junctions[3,4]. Applying a straight line fit to the tunneling current at subgap voltages yields a characteristic resistance R_J. Ratios $R_J/R_N > 20$ and values of $I_cR_J > 30$ mV were obtained. The extremely sharp single-electron tunneling characteristics of these junctions and their size make them particularly effective for use in 55 GHz quasiparticle mixing experiments[12]. AC Josepshon steps due to 55 GHz radiation have been observed at voltages exceeding 5 mV[12].

With increasing critical current density, the hysteresis in the junction IV characteristic is reduced (Figure 3). The shunted junction model[13] predicts a reduction of hysteresis as the parameter

$$\beta = \frac{2\pi}{\Phi_0} I_c R_N^2 C$$

is reduced. The non-linear resistance of real tunnel junctions results in hysteresis in excess of the model prediction due to the large dynamic resistance at subgap voltages ($R_J > R_N$)[14]. Using a power-law model of the quasiparticle characteristic

$$I_{qp} = I_0 (V/V_0)^n$$

allows qualitative study of hysteresis as a function of critical current density[15]. Figure 4 is a plot of hysteresis vs. critical current density for a number of junctions representing both edge and overlap geometries. The data lie, as expected, between the predictions for an ideal tunneling characteristic ($n = \infty$), in which no current flows at subgap voltages, and a parabolic conductance ($n = 2$), which represents large subgap current. (Values for junction capacitance were obtained using published numbers for dielectric constant and oxide thickness of Nb-Pb junctions with rf plasma oxidation[16]). Note that significant reduction of hysteresis does not occur until J_c exceeds 10^4 amp/cm^2, due to the large dielectric constant of Nb_2O_5.

In high J_c junctions, several effects were observed which could be attributed to a non-equilibrium state in one or both junction films. These included a reduction of the energy gap sum, a negative resistance at this voltage, and a transition to the normal state in one of the junction electrodes. Although thorough study of these effects would require a three-film configuration,[17,18] several comments can be made here. Gap reduction and negative resistances at the gap voltage have been seen by several workers,[1,17,18] and are usually attributed to non-equilibrium quasiparticle injection, but simple heating could produce such effects in some situations. We often observed a break in the IV curve of a high J_c device, at voltages above the gap sum, which could be attributed to a normal region in one of the electrodes. It does not appear that this state is due to simple heating since no effect was seen in low J_c junctions, even at much higher levels of power dissipation than required to observe the effect in otherwise identical high J_c junctions. The existence of a non-equilibrium state due to large levels of quasiparticle injection at the gap edge in high J_c junctions could explain all of the observed effects[17,18].

Non-equilibrium effects, either simple heating or quasiparticle injection, could set limits on ultimate useful current densities for tunnel junctions. More study of such limits is desirable. Geometry plays a large role, since efficient removal of heat and non-equilibrium quasiparticles and phonons is important. Edge geometries offer an advantage in this respect,allowing a point contact-like geometry in a thin film tunnel junction. Proper choice of substrate and protective materials may be important[19] (a photoresist coating was used to protect the lead alloy films of devices used in this work during thermal cycling and storage). Careful device construction should minimize non-equilibrium effects, allowing useful devices with J_c in the 10^6 amp/cm^2 range.

Complete removal of hysteresis in a tunnel junction requires either a sizeable leakage current[1] or external shunting. In a low J_c device, the value of shunt resistance (R_s) required to eliminate hysteresis is much smaller than R_N. Almost all current flows in the shunt, effectively shorting the device. Assuming an ideal quasiparticle conductance[15], reduction of β (at subgap voltages) to a value below ≈ 0.8[13] would require a shunt resistance

$$R_s \lesssim 3.2K_\infty R_N,$$

where $K_\infty = \phi_0 I_c / 2\pi C V_0^2$ and V_0 is the gap voltage[15]. In a junction with $J_c = 5 \times 10^5$ amp/cm^2 and linear dimensions of 150 nm, R_N would be around 15Ω. A 50Ω shunt resistance would suffice to remove hysteresis. Thus, attainable values of J_c could lead to a useful class of devices.

In conclusion, we have developed a very flexible process for producing very small tunnel junctions in Nb having a wide range of properties. The high quality of these junctions can be immediately exploited in various Josephson device applications while the attainment of high J_c values, the highest yet reported, allows continued study of the limits of tunnel junction performance.

We are pleased to acknowledge the advice and assistance rendered by Dr. A. C. Callegari in developing the fabrication process and thank him for permission to mention the microwave radiation results. We also wish to acknowledge the expert technical assistance rendered by R. A. Bartynski and C. Toro during this work.

This research was supported in part by ONR.

REFERENCES

1. R. E. Howard, E. L. Hu, L. D. Jackel, L. A. Fetter, and R. H. Bosworth, Appl. Phys. Lett. 35, 879 (1979).
2. R. F. Broom, R. B. Laibowitz, Th. O. Mohr, and W. Walter, IBM J. Res. Develop. 24, 212 (1980).
3. K. Schwidtal, J. Appl. Phys. 43, 202 (1972).
4. R. F. Broom, J. Appl. Phys. 47, 5432 (1976).
5. J. H. Greiner, J. Appl. Phys. 42, 5151 (1971).
6. P. C. Karulkar and J. E. Nordman, J. Vac. Sci. Tech. 17, 462 (1980).
7. P. C. Karulkar and J. E. Nordman, J. Appl. Phys. 50, 7051 (1979).
8. A. W. Kleinsasser and R. A. Buhrman, to be published in the Proceedings of the Ninth International Conference on Electron and Ion Beam Science an Technology, St. Louis, MO. (May 1980).
9. S. K. Lahiri, S. Basavaiah, and C. J. Kircher, Appl. Phys. Lett. 36, 334 (1980).
10. R. H. Havemann, J. Vac. Sci. Tech. 15, 389 (1978).
11. V. Ambegaokar and A. Baratoff, Phys. Rev. Lett. 10, 486 (1963).
12. A. C. Callegari, A. W. Kleinsasser and R. A. Buhrman (to be published).
13. W. C. Stewart, Appl. Phys. Lett. 12, 277 (1968); D. E. McCumber, J. Appl. Phys. 37, 3113 (1968).
14. W. C. Scott, Appl. Phys. Lett. 17, 166 (1970).
15. W. C. Stewart, J. Appl. Phys. 45, 452 (1974).

16. S. Basavaiah and J. H. Greiner, J. Appl. Phys. 47, 4201 (1976).

17. R. C. Dynes, V. Narayanamurti and J. P. Garno, Phys. Rev. Lett. 29, 229 (1977).

18. K. E. Gray and H. W. Willemsen, J. Low Temp. Phys. 31, 911 (1978).

19. S. B. Kaplan, J. Low Temp. Phys. 37, 343 (1979).

FIGURE CAPTIONS

Figure 1 Edge junction fabrication. An Al_2O_3 film is deposited on the Nb base film using argon-oxygen ion beam deposition and lift-off (a). Ion milling through the Nb film leaves a tapered edge protected by Al_2O_3 (b). The counterelectrode completes the junction; one dimension is limited by the Nb film thickness (c). The other dimension is determined by the width of the overlap region (d).

Figure 2 IV characteristic of a low current density (10^3 amp/cm^2) junction.

Figure 3 IV characteristic of a high current density (4×10^5amp/cm^2) junction.

Figure 4 Hysteresis vs. critical current density. The ordinate is the ratio I_R/I_c (Fig. 3). Theoretical curves are for various power-law conductances.

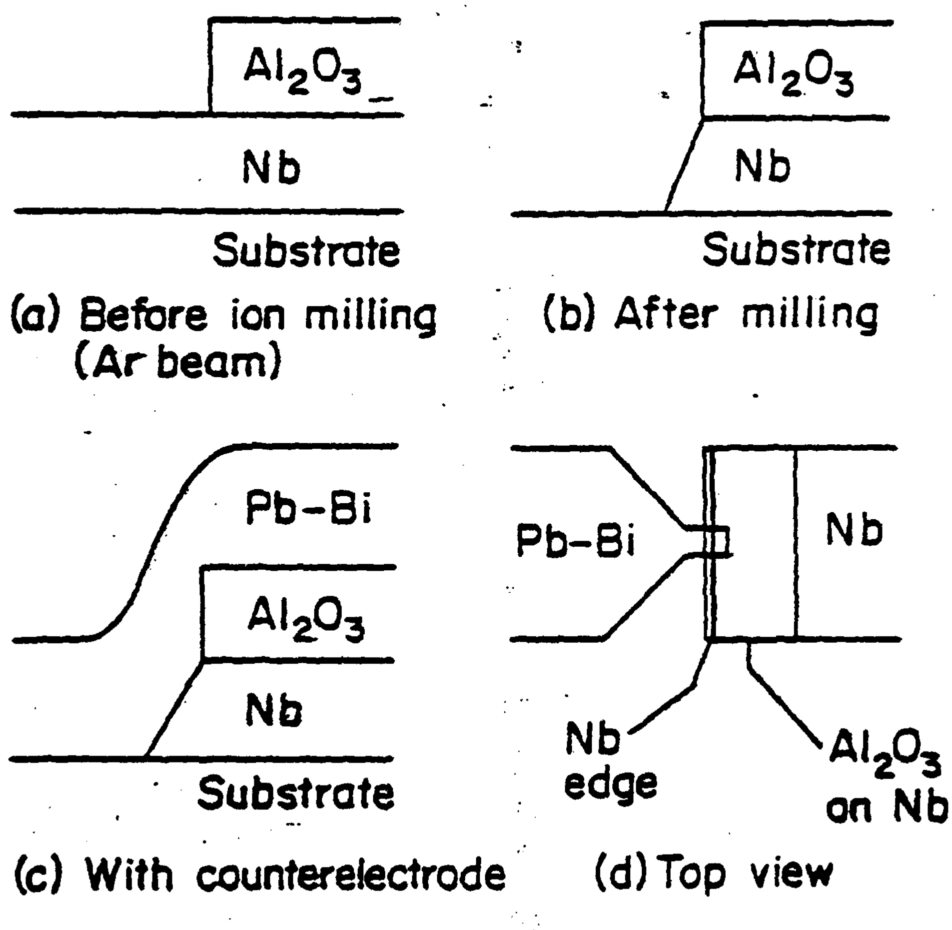

Al_2O_3
Nb
Substrate
(a) Before ion milling
(Ar beam)
Al_2O_3
Nb
Substrate
(b) After milling
Pb-Bi
Al_2O_3
Nb
Substrate
(c) With counterelectrode
Pb-Bi
Nb
Nb
edge
Al_2O_3
on Nb
(d) Top view

FIG. 1

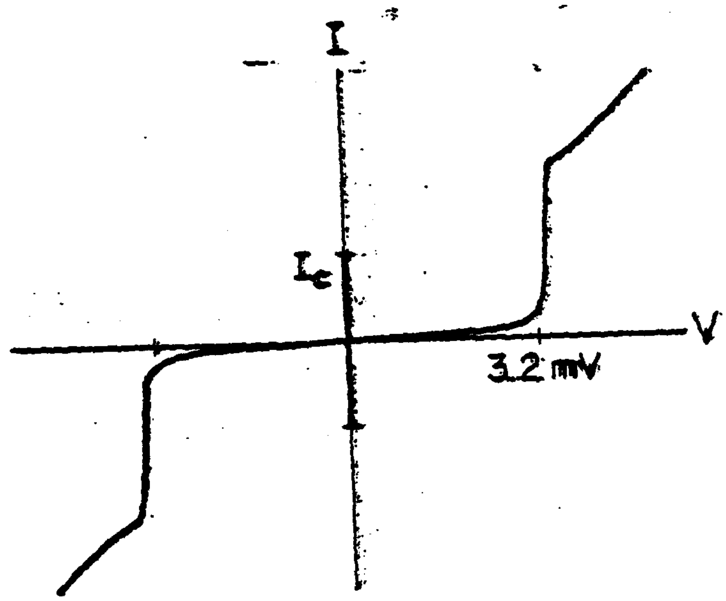

FIG-2

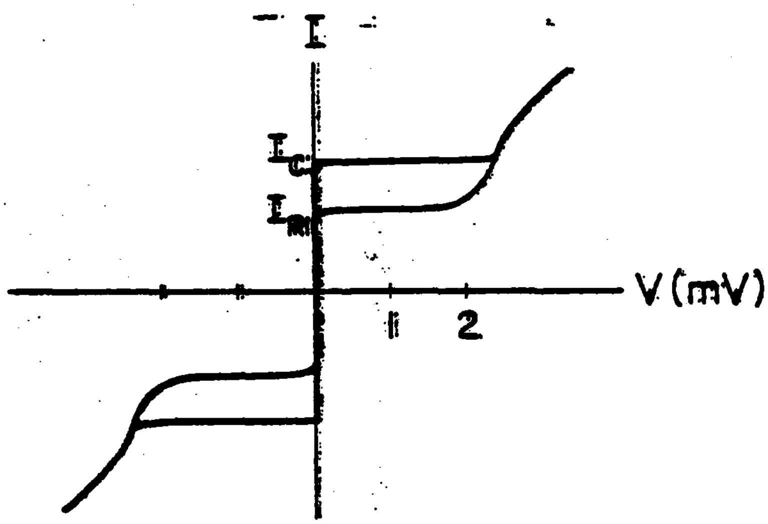

FiG.3

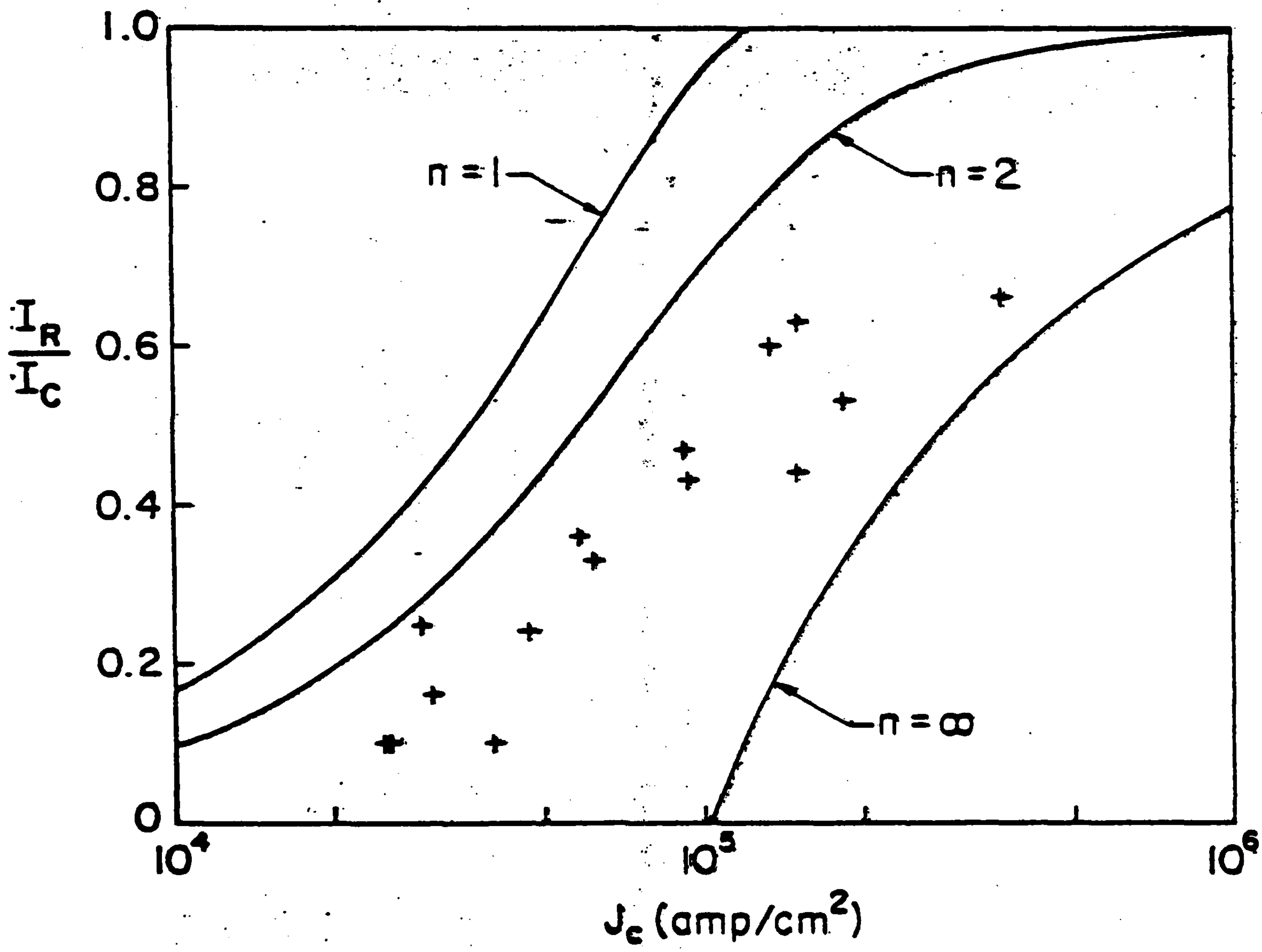

Fig. 4

DAT
FILM